Am J Cancer Res 2022;12(8):3561-3580
www.ajcr.us /ISSN:2156-6976/ajcr0144417

Original Article

Cuproptosis-related gene SLC31A1 is a potential predictor for diagnosis, prognosis and therapeutic response of breast cancer

Xiao Li[1], Zhaosheng Ma[2], Linhang Mei[2]

[1]*Emergency Department, Taizhou Hospital of Zhejiang Province Affiliated to Wenzhou Medical University, Taizhou 317000, Zhejiang, China;* [2]*Department of Oncological Surgery, Taizhou Hospital of Zhejiang Province Affiliated to Wenzhou Medical University, Taizhou 317000, Zhejiang, China*

Received May 27, 2022; Accepted July 16, 2022; Epub August 15, 2022; Published August 30, 2022

Abstract: Cuproptosis is a recently reported novel way of cell death. A comprehensive study regarding expression, function and mechanism of cuproptosis-related genes in breast cancer is still absent. In this work, a series of *in silico* analyses were employed and SLC31A1 was selected as the most potential cuproptosis-related gene in breast cancer, which was statistically upregulated and possessed significant abilities to predict diagnosis, prognosis and drug response. Moreover, SLC31A1 was significantly positively correlated with different immune cell infiltration levels, immune cell biomarkers or immune checkpoints in breast cancer. Upstream G2E3-AS1/let-7a-5p and CDKN2B-AS1/let-7b-5p pathways were found to be responsible for SLC31A1 upregulation in breast cancer based on competing endogenous RNA mechanism. Furthermore, we found that SLC31A1 overexpression might be also induced by its high copy number level in breast cancer. Collectively, our current data elucidated that cuproptosis-related SLC31A1 might be a promising diagnostic/prognostic biomarker and drug responsive predictor in breast cancer.

Keywords: Cuproptosis, copper, SLC31A1, ncRNA, prognosis, breast cancer, bioinformatic analysis

Introduction

Breast cancer is the most common cancer type and is also one of the leading causes of cancer-associated deaths in women all over the world [1]. Huge advances have been achieved during the past decades in the aspects of breast cancer screening, diagnosis, therapy and recurrence monitoring [2]. However, the total outcome of patients with breast cancer is still discontent. Identifying the molecular mechanism of breast carcinogenesis and progression is extremely meaningful for seeking and developing therapeutic targets, thereby improving prognosis of patients with breast cancer.

As is known to all, copper is an important and essential cofactor for all organisms including human body [3]. However, when the copper concentrations have exceeded than a normal threshold, it will be toxic and induce cell death, namely copper-induced cell death called cuproptosis [4]. Several genes are reported to be involved in this process, including FDX1 [3], NLRP3 [5, 6], SLC31A1 [7] and MTF1 [8, 9]. Aberrant regulation of some of these cuproptosis-related genes have been validated to play important roles in cancer initiation and progression [10-12]. However, to date, a comprehensive study regarding the expression, prognosis, diagnosis, immune correlation and mechanism of cuproptosis-related genes in breast cancer is still and need to be further explored.

In this study, a total of 19 cuproptosis-related genes were firstly collected for subsequent research. Next, the expression levels and prognostic and diagnostic values of them were determined and validated in breast cancer. Finally, the dysregulated mechanisms responsible for SLC31A1 overexpression in breast cancer were explored, including ncRNAs, DNA copy number variation and promoter methylation. The findings from this study might provide key clues for identifying and developing effective therapeutic targets and promising biomarkers in breast cancer.

Materials and methods

starBase analysis

starBase (http://starBase.sysu.edu.cn/) [34, 35], a database for decoding miRNA-ceRNA, miRNA-ncRNA and RNA-protein interaction networks from CLIP-Seq data, was used for determine the expression levels of cuproptosis-related genes, miRNAs and lncRNAs in breast cancer. starBase was also employed to assess the expression correlation of SLC31A1-miRNA, SLC31A1-lncRNA, miRNA-lncRNA, SLC31A1-immune checkpoint as well as SLC31A1-immune cell biomarker pairs in breast cancer as previously described [17].

GEPIA analysis

Gene Expression Profiling Interactive Analysis (GEPIA, http://gepia.cancer-pku.cn/) is a recently developed interactive web server for analyzing the RNA sequencing expression data of more than 9,000 tumors and more than 8,000 normal samples from the TCGA and GTEx projects [36]. In this study, GEPIA database was introduced to validate cuproptosis-related genes' expression levels and prognostic values in breast cancer. Moreover, the expression relationship of SLC31A1 with PDCD1, CD274, CTLA4, G2E3-AS1 or CDKN2B-AS1 in breast cancer was also evaluated by GEPIA database. Additionally, GEPIA database was also employed to confirm the correlation of SLC31A1 with various immune cell biomarkers in breast cancer.

Kaplan-Meier plotter analysis

Kaplan-Meier plotter (http://kmplot.com/analysis/) is an online tool for evaluating the effects of genes, miRNAs and lncRNAs in 21 types of human malignancies, which sources was collected from GEO, EGA and TCGA databases [37]. In this study, the prognostic values of cuproptosis-related genes, miRNAs or lncRNAs in breast cancer were determined by Kaplan-Meier plotter database. After entering the molecule names into the webpage, the survival analysis was automatically performed and the Kaplan-Meier plots could be directly downloaded from the online website.

PrognoScan analysis

PrognoScan (http://dna00.bio.kyutech.ac.jp/PrognoScan/) is a new database for meta-survival analysis of genes [38], which was employed for further validating the prognostic value of SLC31A1 in breast cancer as previously reported [20].

ROC curve analysis

Receiver Operating Characteristic (ROC) curve was plotted to represent the diagnostic values of SLC31A1 or its related miRNAs in breast cancer. For SLC31A1, the expression data was downloaded from TCGA database, after which ROC curve analysis was performed by usage of GraphPad Prism software. For miRNAs, ROC curve was automatically drawn by CancerMIRNome (http://bioinfo.jialab-ucr.org/CancerMIRNome), which was an interactive analysis and visualization database [39].

STRING analysis

The interaction among SLC31A1-related genes was explored using STRING (https://cn.string-db.org/cgi/input.pl), which is an online database for customizable protein-protein networks and functional characterization of user-uploaded gene/measurement sets [40]. Only protein-protein pairs with a combined score more than 0.4 were included for subsequent analysis.

CTR-DB analysis

Cancer Treatment Response gene signature Database (CTR-DB, http://ctrdb.ncpsb.org.cn/), a unique tool for basic and clinical researchers to access, integrate and reuse clinical transcriptomes with cancer drug response [41], was employed to determine the effect of SLC31A1 in predicting chemotherapeutic sensitivity in breast cancer.

TIMER analysis

TIMER (http://cistrome.shinyapps.io/timer/) is a web server providing broad use for cancer researchers to comprehensively analyze tumor-infiltrating immune cells [42], which was utilized to assess the correlation of SLC31A1 with tumor infiltrating immune cells, immune checkpoints or immune biomarkers in breast cancer.

cBioPortal analysis

cBioPortal (http://cbioportal.org), a widely-used database for comprehensive analysis of com-

Figure 1. Determination of cuproptosis-related genes in breast cancer by starBase. The expression levels of NFE2L2 (A), NLRP3 (B), ATP7B (C), ATP7A (D), SLC31A1 (E), FDX1 (F), LIAS (G), LIPT1 (H), LIPT2 (I), DLD (J), DLAT (K), PDHA1 (L), PDHB (M), MTF1 (N), GLS (O), CDKN2A (P), DBT (Q), GCSH (R) and DLST (S) in TCGA breast cancer samples compared with TCGA normal breast samples. *P<0.05; ^{ns}P>0.05.

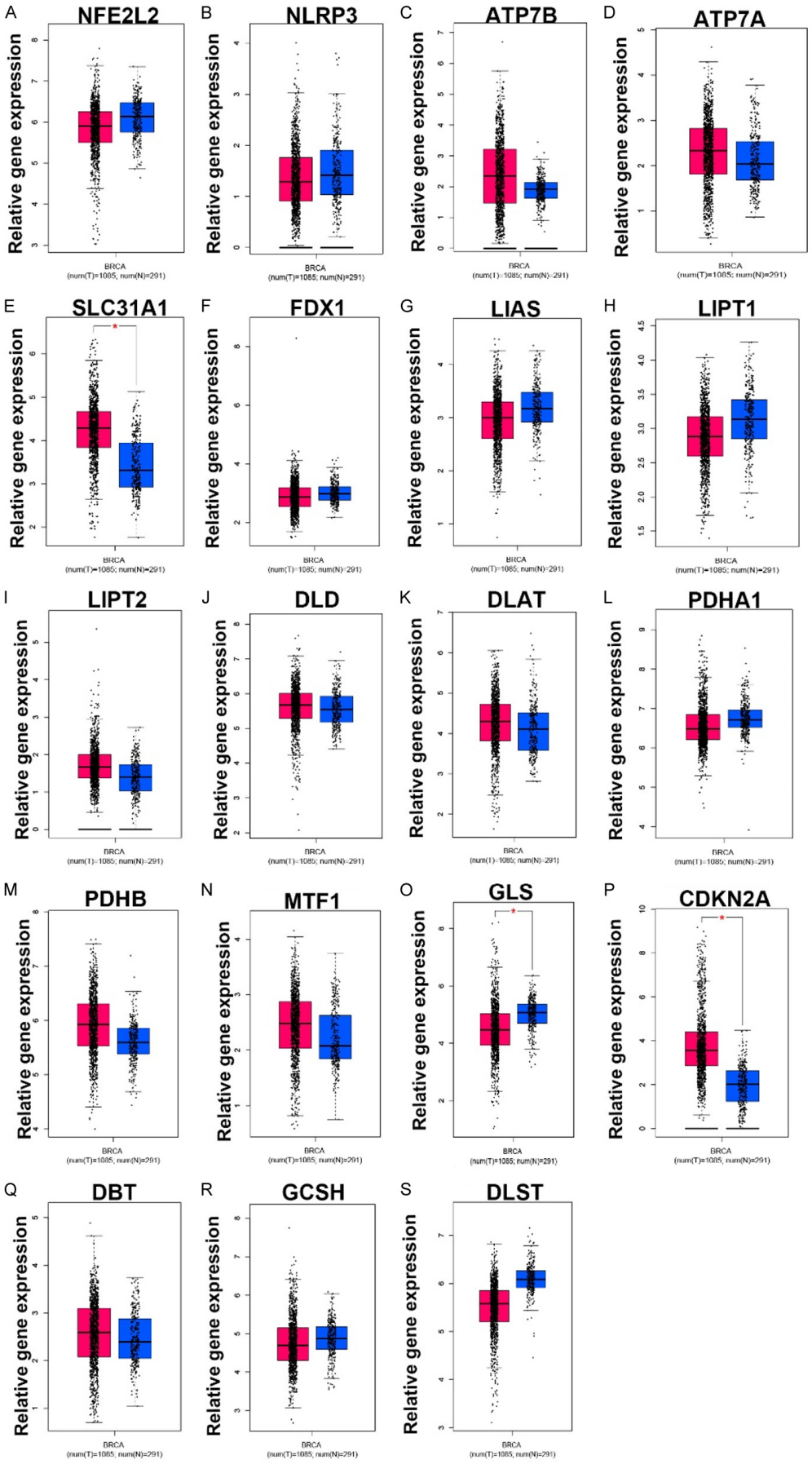
A
NFE2L2
B
NLRP3
C
ATP7B
D
ATP7A
E
SLC31A1
F
FDX1
G
LIAS
H
LIPT1
I
LIPT2
J
DLD
K
DLAT
L
PDHA1
M
PDHB
N
MTF1
O
GLS
P
CDKN2A
Q
DBT
R
GCSH
S
DLST
Relative gene expression
BRCA
(num(T)=1085; num(N)=291)

Figure 2. Validation of cuproptosis-related genes in breast cancer by GEPIA. The expression levels of NFE2L2 (A), NLRP3 (B), ATP7B (C), ATP7A (D), SLC31A1 (E), FDX1 (F), LIAS (G), LIPT1 (H), LIPT2 (I), DLD (J), DLAT (K), PDHA1 (L), PDHB (M), MTF1 (N), GLS (O), CDKN2A (P), DBT (Q), GCSH (R) and DLST (S) in TCGA breast cancer samples compared with GTEx and TCGA normal breast samples. *P<0.05.

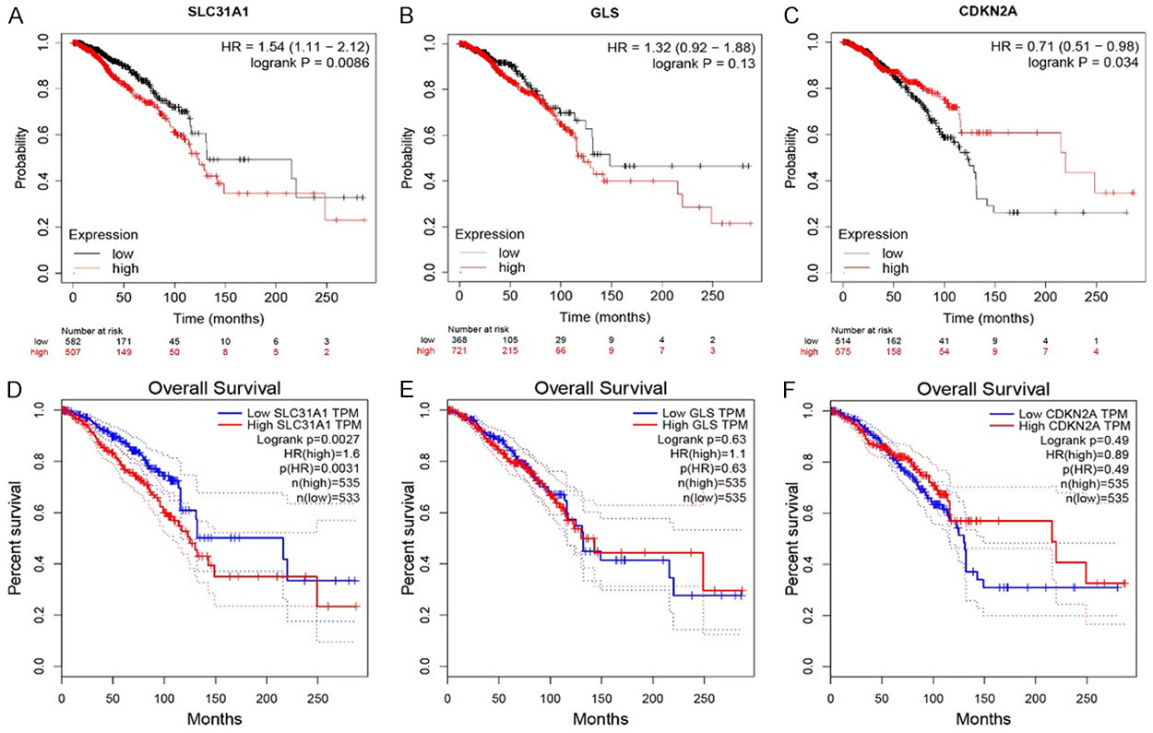

Figure 3. Survival analysis for SLC31A1, GLS and CDKN2A in breast cancer. The prognostic values of SLC31A1 (A), GLS (B) and CDKN2A (C) in breast cancer assessed by Kaplan-Meier plotter. The prognostic values of SLC31A1 (D), GLS (E) and CDKN2A (F) in breast cancer evaluated by GEPIA.

plex cancer genomics and clinical profiles [43], was utilized to determine the relationship between SLC31A1 expression and its DNA copy number or promoter methylation levels in breast cancer.

UALCAN analysis

UALCAN (http://ualcan.path.uab.edu/index.html), a comprehensive, user-friendly, and interactive web resource for analyzing cancer OMICS data [44], was introduced to detect the promoter methylation of SLC31A1 in TCGA breast cancer and normal breast samples.

Statistical analysis

All the statistical analyses in this study were automatically performed by the online databases or tools as mention above. *P*-value <0.05 or logrank *P*-value <0.05 was considered as statistically significant.

Discussion

Cuproptosis is a novel recently-reported way of cell death by partially targeting lipoylated TCA cycle proteins [3]. However, a comprehensive study regarding cuproptosis-related genes' expression, diagnosis, prognosis and mechanisms in breast cancer is still absent and need to be conducted.

In this study, 19 cuproptosis-related genes, including NLRP3 [5, 6], SLC31A1 [7] and MTF1 [8, 9]. By performing expression analysis using several databases, three overexpressed genes in breast cancer, consisting of SLC31A1, GLS and CDKN2A, were selected for following study. After analyzing and confirming the prognostic and diagnostic values of them in breast cancer, SCL31A1 was chosen as the most potential cuproptosis-related gene in breast cancer. Despite no studies about SLC31A1 in breast cancer have been reported, SLC31A1 has been

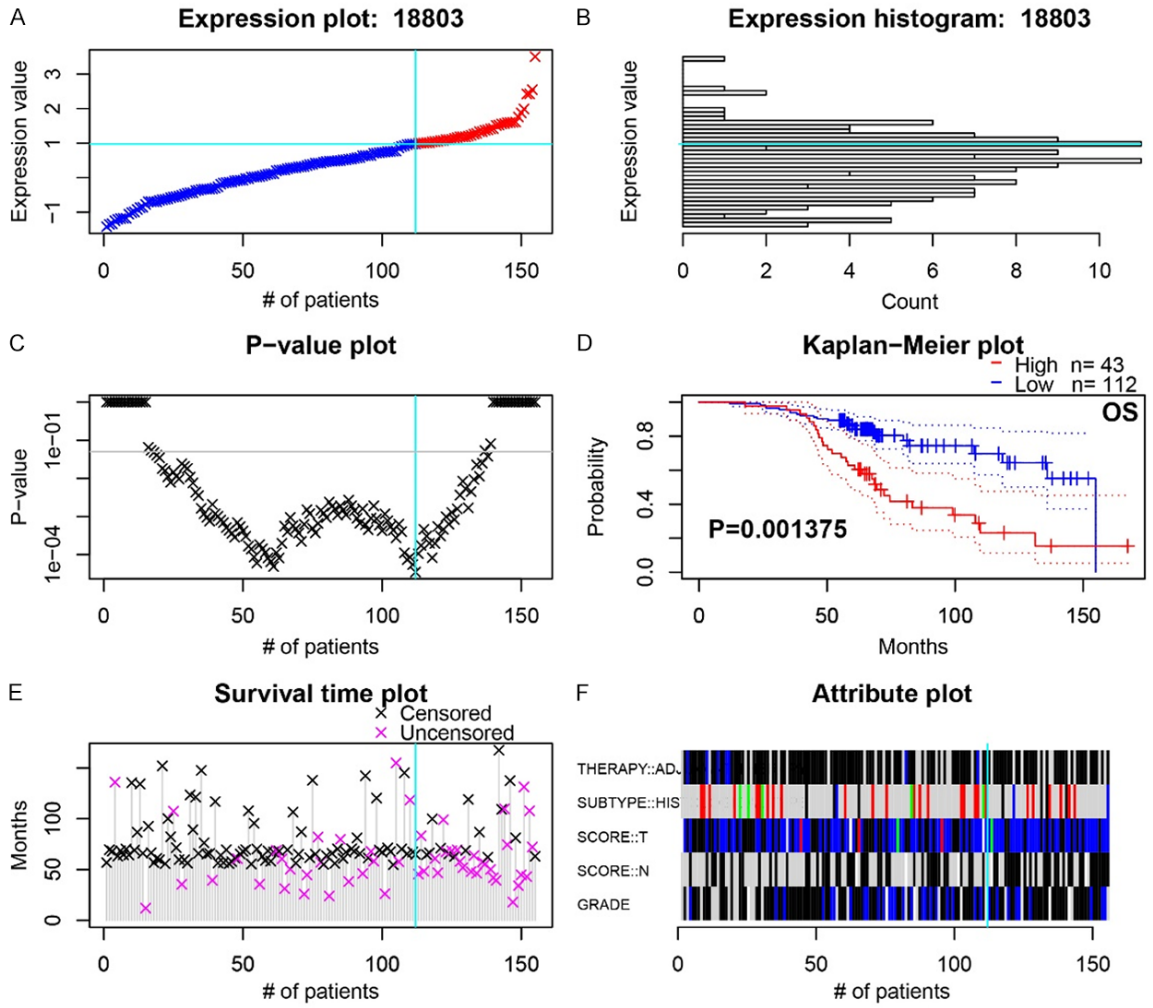

Figure 4. The prognostic value of SLC31A1 in breast cancer validated using GSE9893 dataset. A. The expression plot of SLC31A1 in breast cancer patients of GSE9893 dataset. B. The expression histogram of SLC31A1 in breast cancer patients of GSE9893 dataset. C. The *P*-value plot of SLC31A1 in breast cancer patients of GSE9893 dataset. D. The Kaplan-Meier plot of SLC31A1 in GSE9893 dataset. E. The detailed survival time plot of SLC31A1 in GSE9893 dataset. F. The attribute plot of clinical features of breast cancer patients in GSE9893 dataset.

found to modulate cisplatin resistance in several types of human cancer. For example, Wu *et al*. suggested that SLC31A1 was involved in ZNF711-mediated suppression of cisplatin resistance in epithelial ovarian cancer [10]; Cheng *et al.* indicated that SLC31A1 was linked to PTBP1-caused chemoresistance to cisplatin in osteosarcoma [16]. Thus, we determined the relationship of SLC31A1 with chemotherapeutic sensitivity in breast cancer. The results suggested that SLC31A1 expression was significantly upregulated in chemotherapeutic non-response group and it also might be served as a promising indicator to predict chemotherapeutic sensitivity of breast cancer.

It has been widely acknowledged that tumor immune infiltration and immune checkpoint levels are closely associated with the efficacy of immunotherapy [17, 18]. Therefore, the association of SLC31A1 expression with different infiltrating immune cell levels or corresponding immune cell biomarkers in breast cancer were assessed. The results together suggested that SLC31A1 was significantly positively correlated with tumor infiltrating immune cells in breast cancer. Moreover, SLC31A1 was also positively linked to CD274 and CTLA4 expression, suggesting that regulation of SLC31A1 might be a potential way to improve the efficacy of immunotherapy in breast cancer.

Multiple studies have reported that miRNAs participate in negative modulation of gene expression in various organisms [19-21]. The

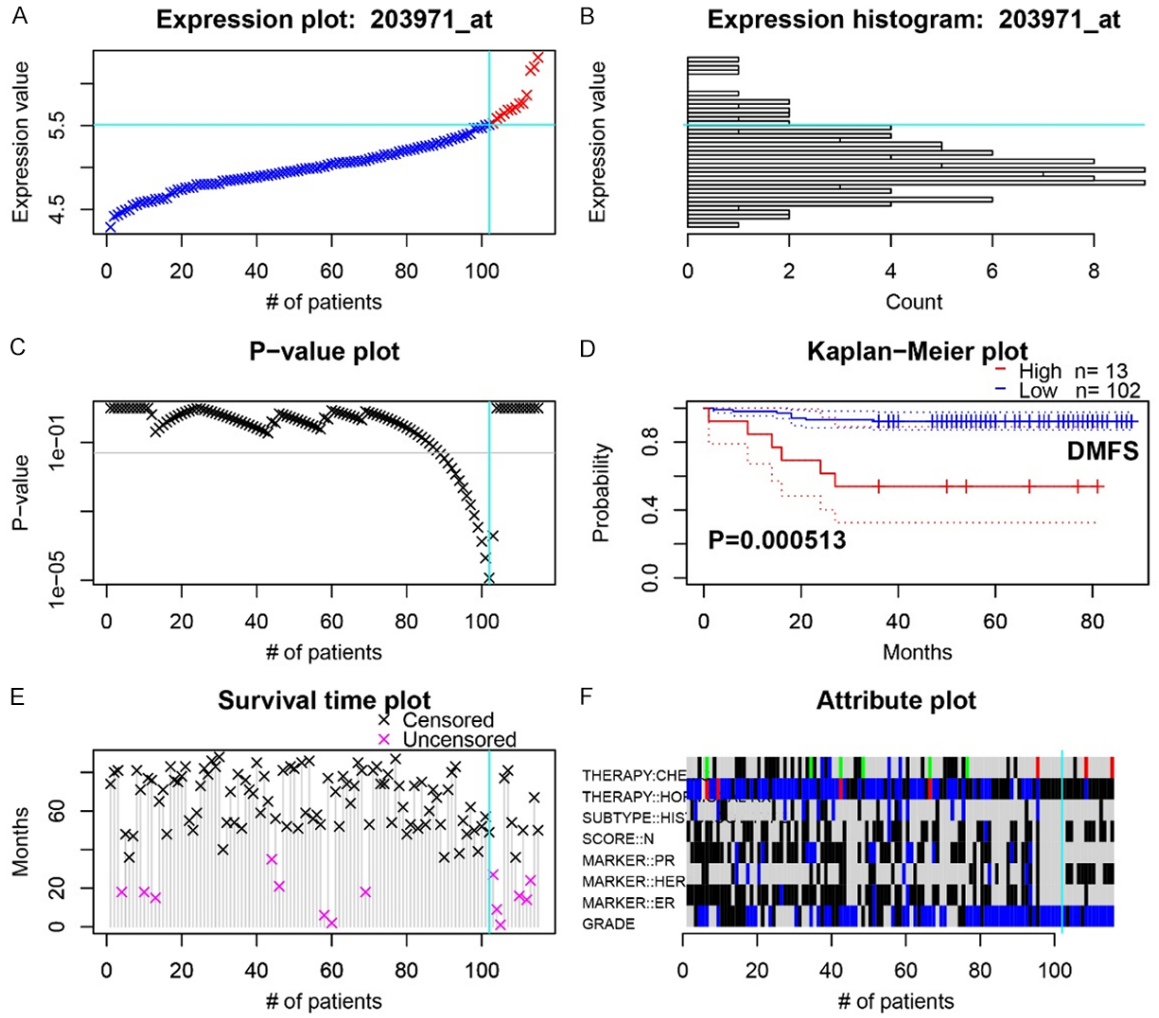

Figure 5. The prognostic value of SLC31A1 in breast cancer validated using GSE19615 dataset. A. The expression plot of SLC31A1 in breast cancer patients of GSE19615 dataset. B. The expression histogram of SLC31A1 in breast cancer patients of GSE19615 dataset. C. The *P*-value plot of SLC31A1 in breast cancer patients of GSE19615 dataset. D. The Kaplan-Meier plot of SLC31A1 in GSE19615 dataset. E. The detailed survival time plot of SLC31A1 in GSE19615 dataset. F. The attribute plot of clinical features of breast cancer patients in GSE19615 dataset.

upstream miRNAs of SLC31A1 were first predicted, after which correlation analysis, expression analysis, ROC curve analysis and survival analysis were performed. By combination of these results, let-7a-5p, let-7b-5p and miR-29a-3p were considered as the most potential upstream binding miRNAs of SLC31A1 in breast cancer. Multiple studies have supported the tumor suppressive effects of the three miRNAs in breast cancer. For example, let-7a-5p could suppressed growth and metastasis of triple-negative breast cancer [22]; let-7b-5p inhibited the cancer-promoting effects of breast cancer-associated fibroblasts [23]; miR-29a-3p hindered MCF-7 cell growth by targeting tumor necrosis factor receptor 1 [24].

Next, the upstream lncRNAs of let-7a-5p, let-7b-5p and miR-29a-3p were forecasted by considering competing endogenous RNA mechanism [25, 26]. After performing correlation analysis, expression analysis and survival analysis, the potential upstream lncRNA G2E3-AS1 of let-7a-5p and CDKN2B-AS1 of let-7b-5p were identified in breast cancer. Previous studies have showed that CDKN2B-AS1 functioned as an oncogenic lncRNA in several human malignancies, including thyroid cancer [27], nasopharyngeal carcinoma [28], endometrial cancer [29], glioma [30] as well as breast cancer [31]. However, no reports regarding G2E3-AS1 in cancer have been found and deserve to be further explored.

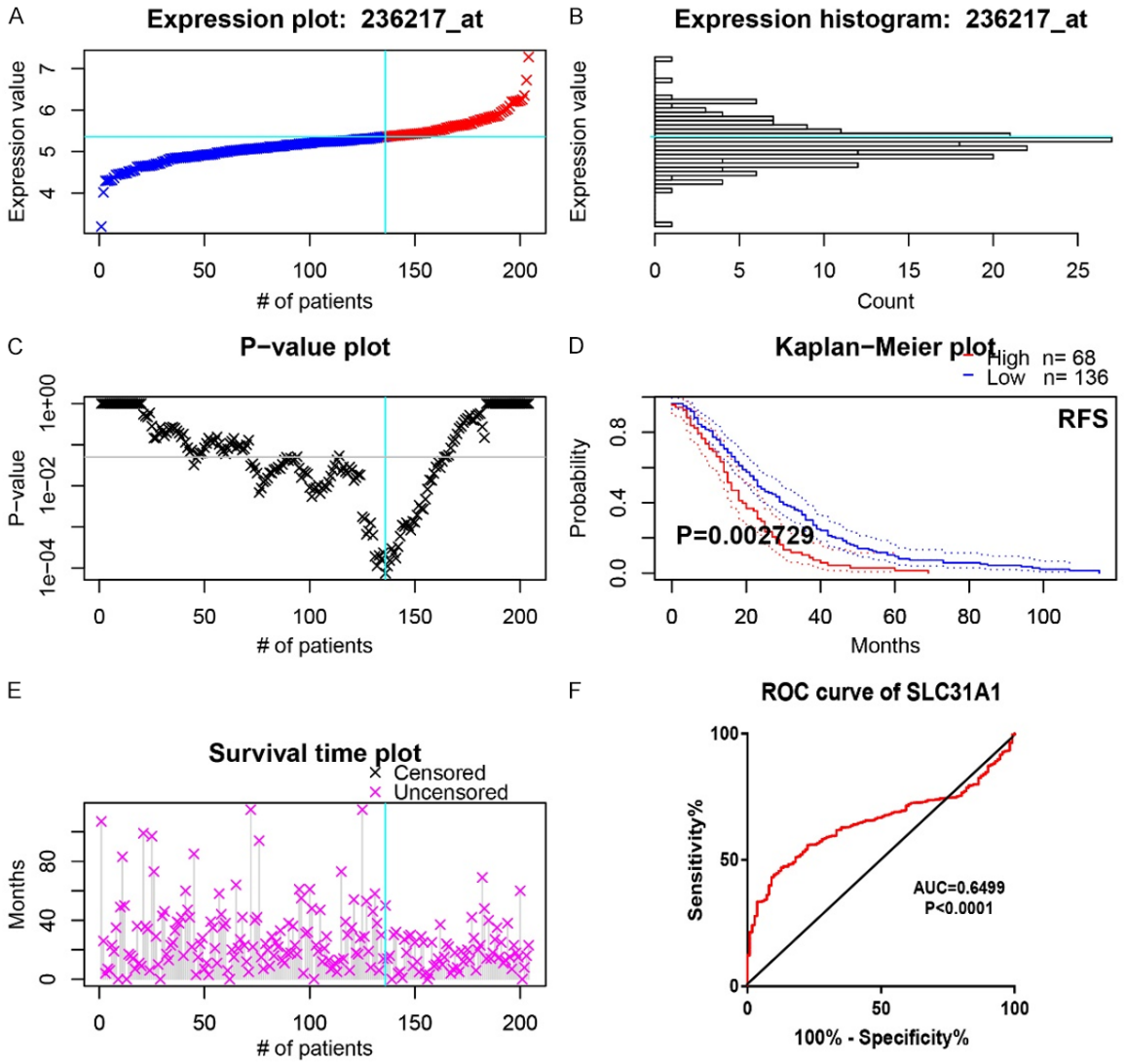

Figure 6. The prognostic value of SLC31A1 in breast cancer validated using GSE12276 dataset and ROC curve analysis for SLC31A1 in breast cancer. A. The expression plot of SLC31A1 in breast cancer patients of GSE12276 dataset. B. The expression histogram of SLC31A1 in breast cancer patients of GSE12276 dataset. C. The *P*-value plot of SLC31A1 in breast cancer patients of GSE12276 dataset. D. The Kaplan-Meier plot of SLC31A1 in GSE12276 dataset. E. The detailed survival time plot of SLC31A1 in GSE12276 dataset. F. The diagnostic value of SLC31A1 in TCGA breast cancer.

Table 1. The expression differences between non-response and response groups and ROC AUCs discriminating the two groups in breast cancer under various therapeutic regimens across CTR-DB datasets

CTR-DB ID	CTR_Microarray_85	CTR_Microarray_57	CTR_Microarray_104
Therapeutic regimen	Cyclophosphamide + Epirubicin + Fluorouracil +Docetaxel	Anthracycline + Taxane	Cyclophosphamide + Epirubicin + Fluorouracil + Paclitaxel
Sample size	16	36	71
LogFC	-0.42	-0.52	-0.33
LogFC *P*-value	0.03	0.03	0.04
AUC	0.85	0.73	0.75
AUC *P*-value	6.1E-03	3.8E-02	8.9E-04

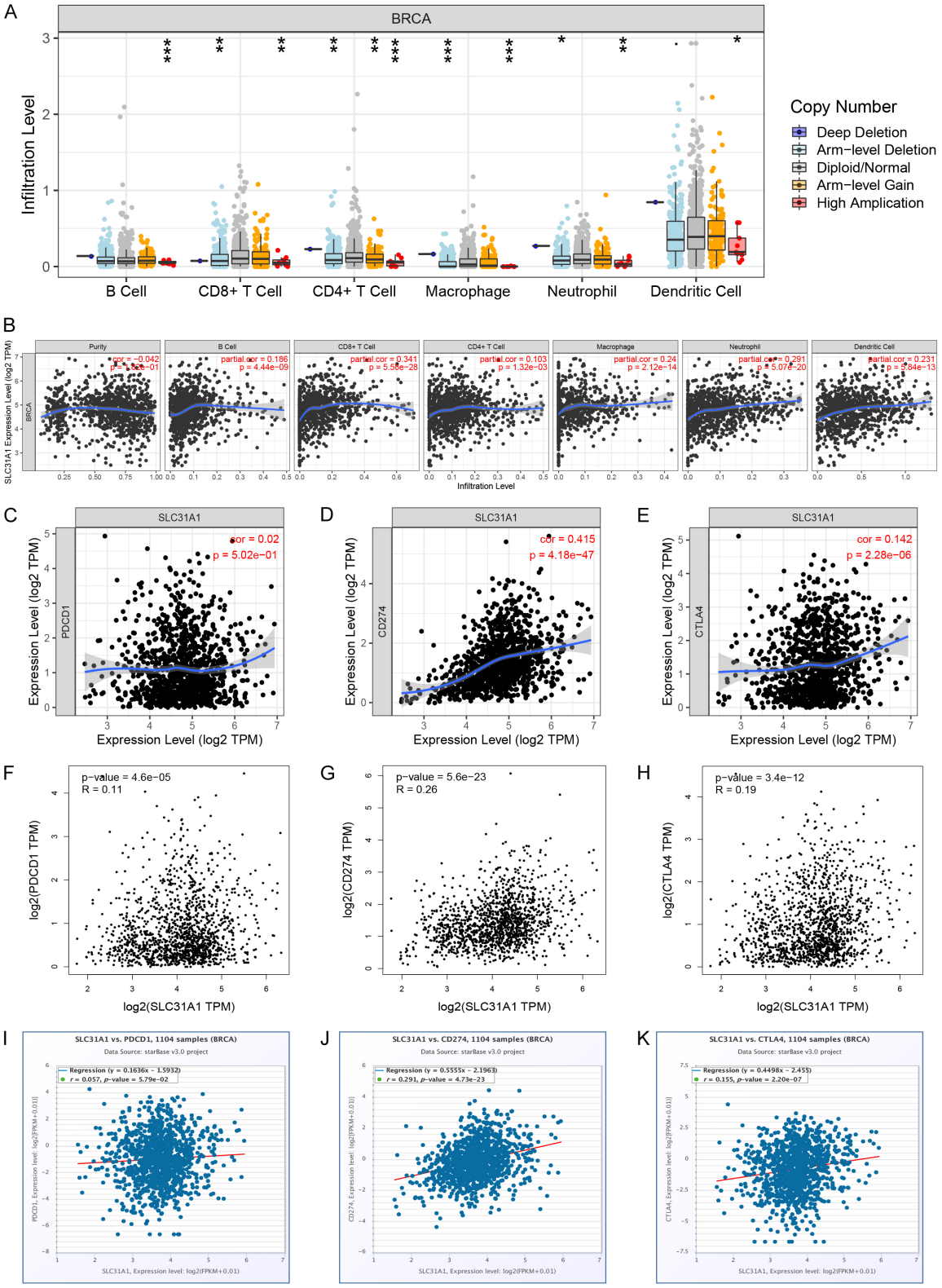

Figure 7. Correlation analysis for SLC31A1 with tumor immune in breast cancer. (A) The infiltration level of different immune cells under various copy numbers of SLC31A1 in breast cancer. (B) The relationship of various immune cell infiltration level with SLC31A1 expression in breast cancer. The expression correlation of SLC31A1 with PDCD1 (C), CD274 (D) and CTLA4 (E) in breast cancer determined by TIMER. The expression correlation of SLC31A1 with PDCD1 (F), CD274 (G) and CTLA4 (H) in breast cancer determined by GEPIA. The expression correlation of SLC31A1 with PDCD1 (I), CD274 (J) and CTLA4 (K) in breast cancer determined by starBase. *P<0.05; **P<0.01; ***P<0.001.

Table 2. Correlation analysis between SLC31A1 and biomarkers of immune cells in breast cancer determined by GEPIA database

Immune cell	Biomarker	R-value	*P*-value
B cell	CD19	0.05	5.3E-02
	CD79A	**0.14**	**2.5E-07*****
CD8+ T cell	CD8A	**0.24**	**1.3E-19*****
	CD8B	**0.18**	**1.6E-11*****
CD4+ T cell	CD4	**0.36**	**9.0E-44*****
M1 Macrophage	NOS2	**0.08**	**2.4E-03****
	IRF5	**0.19**	**9.3E-13*****
	PTGS2	0.00	8.5E-01
M2 Macrophage	CD163	0.01	6.6E-01
	VSIG4	0.00	8.8E-01
	MS4A4A	0.07	7.7E-03
Neutrophil	CEACAM8	-0.22	5.0E-17***
	ITGAM	0.28	8.6E-26***
	CCR7	0.10	1.0E-04***
Dendritic cell	HLA-DPB1	0.23	7.3E-18***
	HLA-DQB1	0.11	2.4E-05***
	HLA-DRA	0.35	9.5E-41***
	HLA-DPA1	0.30	9.6E-31***
	CD1C	0.13	1.7E-06***
	NRP1	0.06	3.0E-02*
	ITGAX	0.17	5.4E-10***

**P*-value <0.05; ***P*-value <0.01; ****P*-value <0.001; The bold values indicate that these results are statistically significant.

Gene copy number variation and aberrant promoter methylation level are closely linked to dysregulation of gene expression [32, 33]. Thus, the relationship of SLC31A1 with its copy number variation or promoter methylation in breast cancer was determined. SLC31A1 expression was markedly positively associated with high copy number level in breast cancer but no significant correlation of SLC31A1 expression with promoter methylation was observed. These findings indicated that SLC31A copy number variation might be another mechanism accounting for SLC31A1 overexpression in breast cancer.

In conclusion, in this study, we identified that SLC31A1 was a potential cuproptosis-related gene in breast cancer, which was markedly upregulated, possessed promising abilities in predicting prognosis, diagnosis and drug sensitivity in breast cancer. Besides, G2E3-AS1/let-7a-5p axis, CDKN2B-AS1/let-7b-5p pathway and high copy number might be responsible for SLC31A1 overexpression in breast cancer. However, these findings should be further validated by much more basic experimental assays and large clinical trials in the future.

Table 3. The expression correlation of SLC31A1 with predicted miRNAs in breast cancer determined by starBase database

miRNA name	R-value	*P*-value
miR-29c-3p	**-0.215**	**7.85E-13**
let-7a-5p	**-0.148**	**1.02E-06**
let-7e-5p	**-0.093**	**2.09E-03**
let-7b-5p	**-0.090**	**3.01E-03**
miR-219a-5p	**-0.080**	**8.43E-03**
miR-506-3p	**-0.076**	**1.20E-02**
miR-139-5p	**-0.066**	**2.88E-02**
miR-29a-3p	**-0.064**	**3.50E-02**
miR-29b-3p	-0.059	5.35E-02
miR-124-3p	-0.051	9.46E-02
miR-375	-0.032	2.87E-01
miR-543	-0.031	3.00E-01
miR-665	-0.024	4.29E-01
miR-371a-5p	-0.020	5.18E-01
miR-132-3p	-0.018	5.51E-01
let-7f-5p	-0.016	6.07E-01
miR-98-5p	-0.007	8.13E-01
miR-212-3p	0.009	7.63E-01
let-7c-5p	0.018	5.64E-01
miR-147a	0.020	5.09E-01
let-7g-5p	0.021	4.86E-01
miR-129-5p	0.030	3.31E-01
miR-425-5p	0.036	2.41E-01
miR-31-5p	0.046	1.29E-01
miR-708-5p	0.055	6.97E-02
let-7i-5p	0.066	2.98E-02
miR-193a-3p	0.072	1.84E-02
miR-28-5p	0.081	7.68E-03
miR-193b-3p	0.083	6.14E-03
miR-196a-5p	0.097	1.43E-03
miR-105-5p	0.104	5.66E-04
let-7d-5p	0.114	1.78E-04
miR-616-3p	0.119	8.65E-05
miR-590-5p	0.144	1.93E-06
miR-505-3p	0.198	4.24E-11
miR-196b-5p	0.203	1.48E-11

The bold values indicate that these results are statistically significant.

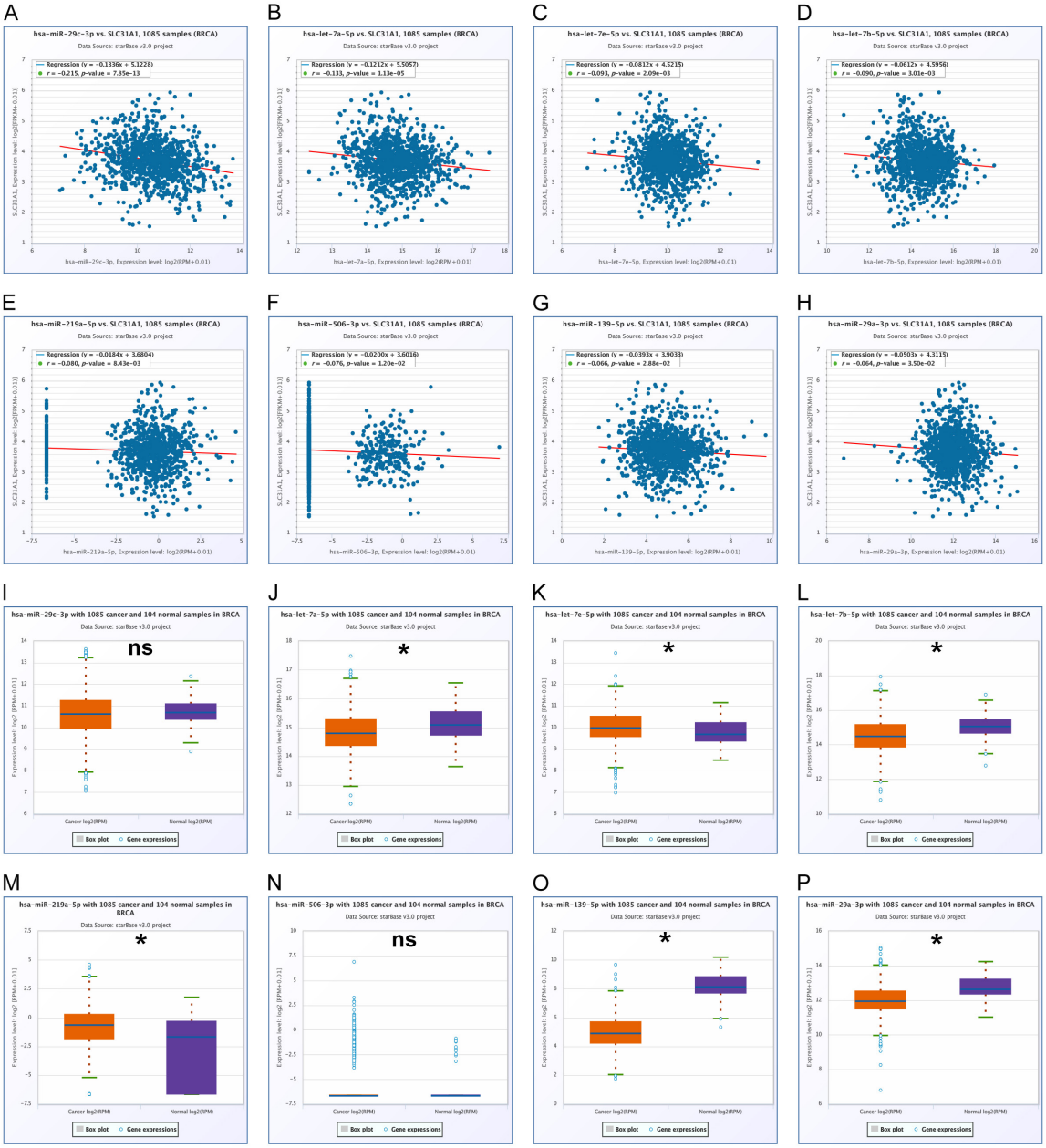

Figure 8. Correlation analysis and expression analysis for the potential miRNAs of SLC31A1 in breast cancer. The expression relationship of SLC31A1 with miR-29c-3p (A), let-7a-5p (B), let-7e-5p (C), let-7b-5p (D), miR-219a-5p (E), miR-506-3p (F), miR-139-5p (G) or miR-29a-3p (H) in breast cancer determined by starBase. The expression levels of miR-29c-3p (I), let-7a-5p (J), let-7e-5p (K), let-7b-5p (L), miR-219a-5p (M), miR-506-3p (N), miR-139-5p (O) or miR-29a-3p (P) in TCGA breast cancer tissues compared with normal breast tissues. *P<0.05; ^{ns}P>0.05.

Results

Expression determination and validation of cuproptosis-related genes in breast cancer

By reviewing the literatures [13-15], a total of 19 cuproptosis-related genes were included for subsequent analysis, consisting of NFE2L2, NLRP3, ATP7B, ATP7A, SLC31A1, FDX1, LIAS, LIPT1, LIPT2, DLD, DLAT, PDHA1, PDHB, MTF1, GLS, CDKN2A, DBT, GCSH and DLST. Firstly, the expression levels of the 19 genes in breast cancer were determined by starBase database. As presented in **Figure 1**, NFE2L2, NLRP3, ATP7A, FDX1, LIAS, LIPT1, LIPT2, DLD, DLAT, PDHA1, MTF1, GLS, DBT, GCSH and DLST were

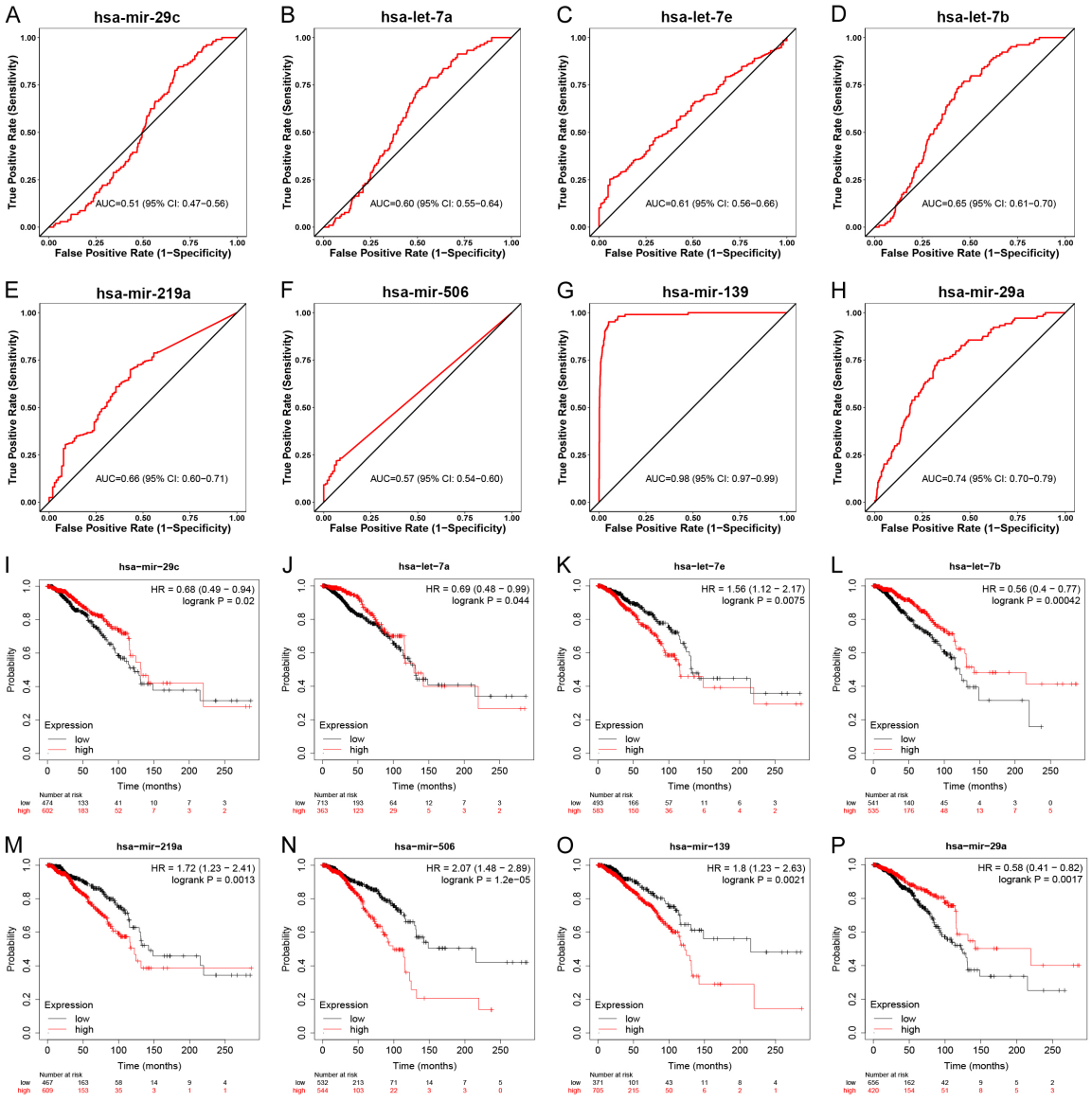

Figure 9. ROC curve analysis and survival analysis for the potential miRNAs of SLC31A1 in breast cancer. The diagnostic values of miR-29c-3p (A), let-7a-5p (B), let-7e-5p (C), let-7b-5p (D), miR-219a-5p (E), miR-506-3p (F), miR-139-5p (G) or miR-29a-3p (H) in breast cancer assessed by CancerMIRNome. The prognostic values of miR-29c-3p (I), let-7a-5p (J), let-7e-5p (K), let-7b-5p (L), miR-219a-5p (M), miR-506-3p (N), miR-139-5p (O) or miR-29a-3p (P) in breast cancer evaluated by Kaplan-Meier plotter.

obviously downregulated but ATP7B, SLC31A1, PDHB and CDKN2A were markedly upregulated in breast cancer when compared with normal controls. For LIPT2, no statistical difference between breast cancer and normal breast samples was observed. Subsequently, GEPIA database was introduced to confirm the expression of cuproptosis-related genes in breast cancer (**Figure 2**). The result indicated that only GLS (**Figure 2O**) was significantly lower and SLC31A1 (**Figure 2E**) and CDKN2A (**Figure 2P**) were statistically higher in breast cancer tissues than that in normal breast tissues. Taken together, GLS, SLC31A1 and CDKN2A might be three most potential genes associated with cuproptosis in breast cancer.

Survival assessment and validation of cuproptosis-related genes in breast cancer

Next, the prognostic values of the three potential cuproptosis-related genes GLS, SLC31A1 and CDKN2A in breast cancer were assessed. Firstly, Kaplan-Meier plotter was employed to perform survival analysis (**Figure 3A-C**). The

Table 4. The expression correlation of let-7a-5p with predicted lncRNAs in breast cancer determined by starBase database

lncRNA	miRNA	R-value	*P*-value
SNHG16	**let-7a-5p**	**-0.174**	**8.52E-09**
TMPO-AS1	**let-7a-5p**	**-0.157**	**1.88E-07**
SNHG4	**let-7a-5p**	**-0.095**	**1.64E-03**
G2E3-AS1	**let-7a-5p**	**-0.084**	**5.51E-03**
LINC00885	**let-7a-5p**	**-0.069**	**2.26E-02**
LINC02432	let-7a-5p	-0.044	1.46E-01
TTTY15	let-7a-5p	-0.038	2.06E-01
HOXA11-AS	let-7a-5p	-0.036	2.37E-01
SNHG12	let-7a-5p	-0.033	2.82E-01
HELLPAR	let-7a-5p	-0.025	4.14E-01
TRG-AS1	let-7a-5p	-0.018	5.57E-01
SLC9A3-AS1	let-7a-5p	-0.016	5.92E-01
LINC01806	let-7a-5p	-0.013	6.63E-01
LINC00294	let-7a-5p	-0.003	9.10E-01
LINC00665	let-7a-5p	-0.002	9.55E-01
LINC01978	let-7a-5p	0.000	9.94E-01
CDKN2B-AS1	let-7a-5p	0.002	9.60E-01
MIR99AHG	let-7a-5p	0.013	6.64E-01
ARHGAP27P1-BPTFP1-KPNA2P3	let-7a-5p	0.018	5.58E-01
KCNQ1OT1	let-7a-5p	0.022	4.62E-01
ZNF571-AS1	let-7a-5p	0.031	3.02E-01
MEG8	let-7a-5p	0.036	2.38E-01
LINC01678	let-7a-5p	0.044	1.47E-01
HCG18	let-7a-5p	0.045	1.41E-01
OLMALINC	let-7a-5p	0.049	1.08E-01
TMEM147-AS1	let-7a-5p	0.051	9.10E-02
LINC01001	let-7a-5p	0.057	6.12E-02
MUC20-OT1	let-7a-5p	0.063	3.73E-02
NUTM2A-AS1	let-7a-5p	0.063	3.80E-02
ZNF337-AS1	let-7a-5p	0.068	2.50E-02
LINC02242	let-7a-5p	0.076	1.21E-02
LINC02381	let-7a-5p	0.077	1.16E-02
IER3-AS1	let-7a-5p	0.102	8.08E-04
VASH1-AS1	let-7a-5p	0.107	3.96E-04
UBL7-AS1	let-7a-5p	0.116	1.36E-04
LMCD1-AS1	let-7a-5p	0.123	5.19E-05
LINC00265	let-7a-5p	0.123	5.15E-05
NEAT1	let-7a-5p	0.131	1.57E-05
DRAIC	let-7a-5p	0.135	7.99E-06
RPARP-AS1	let-7a-5p	0.136	7.19E-06
LINC00894	let-7a-5p	0.143	2.42E-06
CARMN	let-7a-5p	0.149	8.14E-07
OIP5-AS1	let-7a-5p	0.155	3.09E-07
HEIH	let-7a-5p	0.164	6.06E-08
STAG3L5P-PVRIG2P-PILRB	let-7a-5p	0.168	2.69E-08

result indicated that breast cancer patients with higher expression of SLC31A1 but with lower expression of CDKN2A had poorer prognosis. However, no statistical prognostic value of GLS in breast cancer was observed. Subsequently, GEPIA was used to validate the prognostic roles of the three cuproptosis-related genes in breast cancer (**Figure 3D-F**). Only increased expression of SLC31A1 indicated significant unfavorable prognostic value in breast cancer. By combination of the results from the two databases, SLC31A1 might be the most potential cuproptosis-related gene in breast cancer, which may be also a promising unfavorable prognostic biomarker. Finally, three GEO datasets, consisting of GSE9893, GSE19615 and GSE12276, were introduced to further confirm the predictive value of SLC31A1 in prognosis of breast cancer. The results presented that breast cancer patients with high expression of SLC31A1 had poor overall survival (**Figure 4**), distant metastasis free survival (**Figure 5**) and relapse free survival (**Figure 6A-E**). Taken together, all these findings suggest that SLC31A1 might be an unfavorable prognostic biomarker in breast cancer.

ROC curve analysis for SLC31A1 in breast cancer

In order to assess the diagnostic value of SLC31A1 in breast cancer, ROC curve of SLC31A1 was plotted by usage of TCGA breast cancer and normal breast samples. As shown in **Figure 6F**, SLC31A1 had the significant ability to distinguish breast cancer tissues from normal breast tissues, with AUC value equal to 0.6499 ($P<0.0001$), indicating that SLC31A1 might be also a promising diagnostic biomarker in breast cancer.

Protein-protein interaction (PPI) network and enrichment analysis for SLC31A1

To better understand the molecular action mechanism of SLC31A1, a PPI

LINC00963	let-7a-5p	0.169	1.94E-08
IQCH-AS1	let-7a-5p	0.174	8.61E-09
XIST	let-7a-5p	0.178	3.82E-09
THSD4-AS1	let-7a-5p	0.180	2.31E-09
MIR29B2CHG	let-7a-5p	0.183	1.21E-09
ZNF436-AS1	let-7a-5p	0.185	8.33E-10
TTC28-AS1	let-7a-5p	0.224	7.73E-14
MIRLET7BHG	let-7a-5p	0.311	9.43E-26

The bold values indicate that these results are statistically significant.

Table 5. The expression correlation of let-7b-5p with predicted lncRNAs in breast cancer determined by starBase database

lncRNA	miRNA	R-value	*P*-value
SNHG12	**let-7b-5p**	**-0.266**	**4.66E-19**
TMPO-AS1	**let-7b-5p**	**-0.204**	**1.12E-11**
ARHGAP27P1-BPTFP1-KPNA2P3	**let-7b-5p**	**-0.198**	**4.68E-11**
TMEM147-AS1	**let-7b-5p**	**-0.172**	**1.13E-08**
SLC9A3-AS1	**let-7b-5p**	**-0.157**	**1.98E-07**
SNHG4	**let-7b-5p**	**-0.149**	**8.19E-07**
SNHG16	**let-7b-5p**	**-0.149**	**8.58E-07**
TRG-AS1	**let-7b-5p**	**-0.138**	**5.10E-06**
LINC01978	**let-7b-5p**	**-0.138**	**5.27E-06**
CDKN2B-AS1	**let-7b-5p**	**-0.107**	**4.18E-04**
STAG3L5P-PVRIG2P-PILRB	**let-7b-5p**	**-0.103**	**6.97E-04**
LINC00885	**let-7b-5p**	**-0.08**	**8.41E-03**
HELLPAR	**let-7b-5p**	**-0.071**	**2.02E-02**
LINC00294	**let-7b-5p**	**-0.067**	**2.67E-02**
LINC01678	**let-7b-5p**	**-0.067**	**2.81E-02**
HOXA11-AS	**let-7b-5p**	**-0.065**	**3.21E-02**
MUC20-OT1	let-7b-5p	-0.059	5.08E-02
G2E3-AS1	let-7b-5p	-0.059	5.20E-02
VASH1-AS1	let-7b-5p	-0.057	5.86E-02
LINC02432	let-7b-5p	-0.054	7.32E-02
LINC00665	let-7b-5p	-0.042	1.63E-01
LINC01806	let-7b-5p	-0.037	2.24E-01
LINC00894	let-7b-5p	-0.034	2.67E-01
TTTY15	let-7b-5p	-0.033	2.72E-01
ZNF571-AS1	let-7b-5p	-0.025	4.10E-01
HCG18	let-7b-5p	-0.024	4.24E-01
MIR99AHG	let-7b-5p	-0.016	5.96E-01
LINC02242	let-7b-5p	-0.006	8.33E-01
ZNF436-AS1	let-7b-5p	0.006	8.47E-01
NUTM2A-AS1	let-7b-5p	0.006	8.36E-01
RPARP-AS1	let-7b-5p	0.008	8.00E-01
MEG8	let-7b-5p	0.012	6.83E-01
IER3-AS1	let-7b-5p	0.014	6.56E-01
NEAT1	let-7b-5p	0.020	5.15E-01
LINC02381	let-7b-5p	0.023	4.46E-01

sub-network was constructed by conducting PPI network analysis using STRING database. As presented in Figure S1A, SLC31A1 could interact with CP, CCS, ZBED3, ATOX1, SLC22A2, ATP7B, MTF1, SLC11A2, ATP7A and COX17. Subsequently, Gene Ontology (GO) enrichment analysis for these SLC31A1-related genes in the established sub-network was performed. Two GO categories, involving biological process (BP) and molecular function (MF), were included. As suggested in Figure S1B, the top five enriched items for BP were copper ion export, protein maturation by copper ion transfer, copper ion transmembrane transport, copper ion import and copper ion transport. For MF category, copper transmembrane transporter activity, copper chaperone activity, copper ion transmembrane transporter activity, copper-dependent protein binding and superoxide dismutase copper chaperone activity were the top five enriched items (Figure S1C).

The role of SLC31A1 in predicting chemotherapeutic response in breast cancer

Considering the high expression and promising prognostic and diagnostic values of SLC31A1 in breast cancer, the effect of SLC31A1 in relation with chemotherapeutic sensitivity should be further determined. In this part, three drug trials from CTR-DB database were collected for this analysis, including CEF (cyclophosphamide, epirubicin, Fluorouracil) plus docetaxel, AT (anthracycline, taxane) and CEF (cyclophosphamide, epirubicin, Fluorouracil) plus paclitaxel, which were widely used in clinical practice. As listed in **Table 1**, SLC31A1 expression was significantly decreased in non-response group compared with response group in all the three drug trials. Moreover, SLC31A1 possessed the statistical abilities to distinguish non-response groups from response groups. These findings indicated that high expression of SLC31A1 might be negatively correlated with sensitivity

LINC00963	let-7b-5p	0.038	2.06E-01
LINC01001	let-7b-5p	0.039	1.97E-01
OLMALINC	let-7b-5p	0.042	1.63E-01
TTC28-AS1	let-7b-5p	0.047	1.19E-01
HEIH	let-7b-5p	0.051	9.59E-02
ZNF337-AS1	let-7b-5p	0.051	9.01E-02
LINC00265	let-7b-5p	0.054	7.48E-02
CARMN	let-7b-5p	0.059	5.36E-02
KCNQ1OT1	let-7b-5p	0.065	3.35E-02
LMCD1-AS1	let-7b-5p	0.091	2.80E-03
UBL7-AS1	let-7b-5p	0.097	1.45E-03
IQCH-AS1	let-7b-5p	0.143	2.14E-06
DRAIC	let-7b-5p	0.153	4.22E-07
THSD4-AS1	let-7b-5p	0.168	2.83E-08
MIR29B2CHG	let-7b-5p	0.172	1.19E-08
XIST	let-7b-5p	0.179	2.86E-09
MIRLET7BHG	let-7b-5p	0.283	1.97E-21
OIP5-AS1	let-7b-5p	0.292	1.06E-22

The bold values indicate that these results are statistically significant.

Table 6. The expression correlation of miR-29a-3p with predicted lncRNAs in breast cancer determined by starBase database

lncRNA	miRNA	R-value	*P*-value
LINC01521	**miR-29a-3p**	**-0.196**	**7.09E-11**
OIP5-AS1	**miR-29a-3p**	**-0.125**	**3.74E-05**
CRNDE	**miR-29a-3p**	**-0.115**	**1.48E-04**
MIR193BHG	**miR-29a-3p**	**-0.112**	**2.22E-04**
EBLN3P	**miR-29a-3p**	**-0.086**	**4.82E-03**
TUG1	**miR-29a-3p**	**-0.079**	**9.32E-03**
NPTN-IT1	**miR-29a-3p**	**-0.062**	**4.07E-02**
LINC01224	miR-29a-3p	-0.041	1.76E-01
HCG18	miR-29a-3p	-0.035	2.46E-01
MIR4458HG	miR-29a-3p	-0.033	2.74E-01
CCDC144NL-AS1	miR-29a-3p	-0.027	3.79E-01
LINC00879	miR-29a-3p	-0.021	4.89E-01
LINC00638	miR-29a-3p	-0.021	4.83E-01
DNAAF4-CCPG1	miR-29a-3p	-0.021	4.90E-01
H19	miR-29a-3p	-0.006	8.53E-01
DNAJC27-AS1	miR-29a-3p	0.001	9.73E-01
DUXAP8	miR-29a-3p	0.001	9.74E-01
LIFR-AS1	miR-29a-3p	0.011	7.14E-01
KCNQ1OT1	miR-29a-3p	0.013	6.72E-01
XIST	miR-29a-3p	0.013	6.73E-01
NOP14-AS1	miR-29a-3p	0.015	6.31E-01
MIR29B2CHG	miR-29a-3p	0.019	5.26E-01
PVT1	miR-29a-3p	0.034	2.58E-01
LINC00511	miR-29a-3p	0.057	5.84E-02

of these chemotherapeutic regimens in breast cancer.

The relationship of SLC31A1 with infiltrating immune cells or immune checkpoints in breast cancer

Next, the correlation of SLC31A1 with tumor immune infiltration in breast cancer was also evaluated. As shown in **Figure 7A**, in general, the infiltration levels of immune cells were gradually growing with the increase of the copy number of SLC31A1. SLC31A1 expression was significantly linked to B cell, CD8 positive T cell, CD4 positive T cell, macrophage cell, neutrophil cell and dendritic cell infiltration levels (**Figure 7B**). Moreover, correlation analysis for SLC31A1 with biomarkers of immune cells revealed that SLC31A1 was significantly positively correlated with multiple immune cell's biomarkers (**Table 2**). Immune checkpoint was closely linked to immunotherapeutic effect and immune escape. Therefore, we also determined the relationship between SLC31A1 and immune checkpoints (PDCD1, CD274 and CTLA4). Three databases, consisting of TIMER (**Figure 7C-E**), GEPIA (**Figure 7F-H**) and starBase (**Figure 7I-K**), were employed for this analysis. The results indicated that SLC31A1 expression was markedly positively associated with CD274 or CTLA4 levels in breast cancer.

Prediction and analysis of upstream miRNAs of SLC31A1 in breast cancer

Lots of lines of evidence have well documented that miRNAs are involved in negative regulation of target genes. To ascertain if SLC31A1 is modulated by corresponding miRNAs, the upstream miRNAs of SLC31A1 were predicted. Consequently, a total of 36 possible miRNAs of SLC31A1 were obtained. Correlation analysis suggested that SLC31A1 was markedly negatively correlated with 8 miRNAs in breast cancer as listed in **Table 3** and **Figure 8A-H**. Expression determination for the 8 miRNAs was subsequently conduct-

MIR4697HG	miR-29a-3p	0.066	2.99E-02
HOXA10-AS	miR-29a-3p	0.069	2.31E-02
NEAT1	miR-29a-3p	0.079	9.49E-03
THUMPD3-AS1	miR-29a-3p	0.083	5.94E-03
PCBP1-AS1	miR-29a-3p	0.092	2.44E-03
AFDN-DT	miR-29a-3p	0.098	1.17E-03
MIRLET7BHG	miR-29a-3p	0.108	3.73E-04
HOXA-AS3	miR-29a-3p	0.112	2.07E-04
MIR646HG	miR-29a-3p	0.112	2.17E-04
RAD51-AS1	miR-29a-3p	0.113	1.88E-04
VASH1-AS1	miR-29a-3p	0.117	1.08E-04
MIR762HG	miR-29a-3p	0.124	4.25E-05
SNHG17	miR-29a-3p	0.128	2.48E-05
SNHG20	miR-29a-3p	0.14	3.94E-06
LINC01907	miR-29a-3p	0.144	1.88E-06
ARRDC1-AS1	miR-29a-3p	0.144	2.02E-06
LINC01578	miR-29a-3p	0.167	2.94E-08
LINC01270	miR-29a-3p	0.181	1.85E-09
MIAT	miR-29a-3p	0.183	1.23E-09
GAS5	miR-29a-3p	0.195	8.96E-11
STAG3L5P-PVRIG2P-PILRB	miR-29a-3p	0.198	4.93E-11
SNHG15	miR-29a-3p	0.199	4.08E-11
LINC00689	miR-29a-3p	0.21	3.01E-12
HCP5	miR-29a-3p	0.224	8.91E-14
LINC00852	miR-29a-3p	0.229	2.24E-14
LINC00943	miR-29a-3p	0.257	7.13E-18
MIR497HG	miR-29a-3p	0.267	3.71E-19
FAM30A	miR-29a-3p	0.322	1.46E-27

The bold values indicate that these results are statistically significant.

ed (**Figure 8I-P**). 4 miRNAs (let-7a-5p, let-7b-5p, miR-139-5p and miR-29-3p) and 2 miRNAs (let-7e-5p and miR-219a-5p) were significantly downregulated and upregulated in breast cancer tissues when compared with normal controls. In addition, ROC curve analysis for the 8 miRNAs was conducted to assess their diagnostic values in breast cancer (**Figure 9A-H**). Among the 8 miRNAs, let-7a-5p (AUC=0.60), let-7e-5p (AUC=0.61), let-7b-5p (AUC=0.65), miR-219a-5p (AUC=0.66), miR-139-5p (AUC=0.98) and miR-29a-3p (AUC=0.74) possessed potential diagnostic values in breast cancer. Survival analysis for the 8 miRNAs suggested that breast cancer patients with high expression of miR-29c-3p, let-7a-5p, let-7b-5p and miR-29a-3p but with low expression of let-7e-5p, miR-219a-5p, miR-506-3p and miR-139-5p had favorable prognosis (**Figure 9I-P**). Taken together, let-7a-5p, let-7b-5p and miR-29a-3p might be the three most potential upstream binding miRNAs of SLC31A1 in breast cancer.

Prediction and analysis of upstream lncRNAs of miRNA/SLC31A1 axis in breast cancer

Subsequently, the upstream lncRNAs of let-7a-5p, let-7b-5p and miR-29a-3p were predicted. A total of 53, 53 and 52 possible lncRNAs were predicted to bind to let-7a-5p, let-7b-5p and miR-29a-3p, respectively. As listed in **Tables 4**-**6**, let-7a-5p, let-7b-5p and miR-29a-3p expression were significantly negatively correlated with 5 (SNHG16, TMPO-AS1, SNHG4, G2E3-AS1 and LINC00885), 16 (SNHG12, TMPO-AS1, ARHGAP27P1-BPTFP1-KPNA2P3, TMEM147-AS1, SLC7A3-AS1, SNHG4, SNHG16, TRG-AS1, LINC01978, CDKN2B-AS1, STAG3L5P-PVRIG2P-PILRB, LINC00885, HELLPAR, LINC00294, LINC01678 and HOXA11-AS) and 7 (LINC01521, OIP5-AS1, CRNDE, MIR193BHG, EBLN3P, TUG1 and NPTN-IT1) lncRNAs in breast cancer, respectively. Next, expression analysis for these lncRNAs in breast cancer was performed as suggested in **Figure 10A**. The prognostic values of upregulated lncRNAs in breast cancer were also evaluated (**Figure 10B-K**). The results demonstrated that breast cancer patients with higher expression of G2E3-AS1 (**Figure 10D**) and CDKN2B-AS1 (**Figure 10H**) and with lower expression of SNHG12 (**Figure 10E**) had poorer prognosis. Furthermore, the expression SLC31A1 was statistically positively correlated with G2E3-AS1 (**Figure 10L**) or CDKN2B-AS1 (**Figure 10M**) expression in breast cancer.

The correlation of SLC31A1 expression with its copy number variation or promoter methylation in breast cancer

Other dysregulated mechanisms that might be responsible for SLC31A1 overexpression in breast cancer were also explored. Firstly, the relationship of SLC31A1 expression with copy number variations in breast cancer was determined by usage of TCGA and METABRIC data. We found that SLC31A1 was significantly posi-

A

lncRNA	SNHG16	TMPO-AS1	SNHG4	G2E3-AS1	LINC00885	SNHG12	27P1-BPTFP1-	TMEM147-AS1
Fold change	1.23	3.22	0.86	3.38	1.07	1.32	0.84	1.08
P-value	3.00E-02	2.20E-63	1.60E-01	4.30E-02	5.50E-01	3.20E-03	1.70E-06	8.70E-01
lncRNA	SLC9A3-AS1	TRG-AS1	LINC01978	CDKN2B-AS1	L5P-PVRIG2P-	HELLPAR	LINC00294	LINC01678
Fold change	1.58	1.09	3.51	3.79	0.99	1.11	0.82	0.93
P-value	3.40E-02	6.40E-02	6.40E-20	6.80E-36	1.30E-01	3.70E-01	6.30E-10	1.10E-01
lncRNA	HOXA11-AS	LINC01521	OIP5-AS1	CRNDE	MIR193BHG	EBLN3P	TUG1	NPTN-IT1
Fold change	2.46	1.33	0.78	1.30	0.49	1.18	1.00	0.60
P-value	1.20E-04	8.50E-02	4.60E-13	6.40E-06	4.60E-18	2.00E-02	8.50E-01	2.20E-14

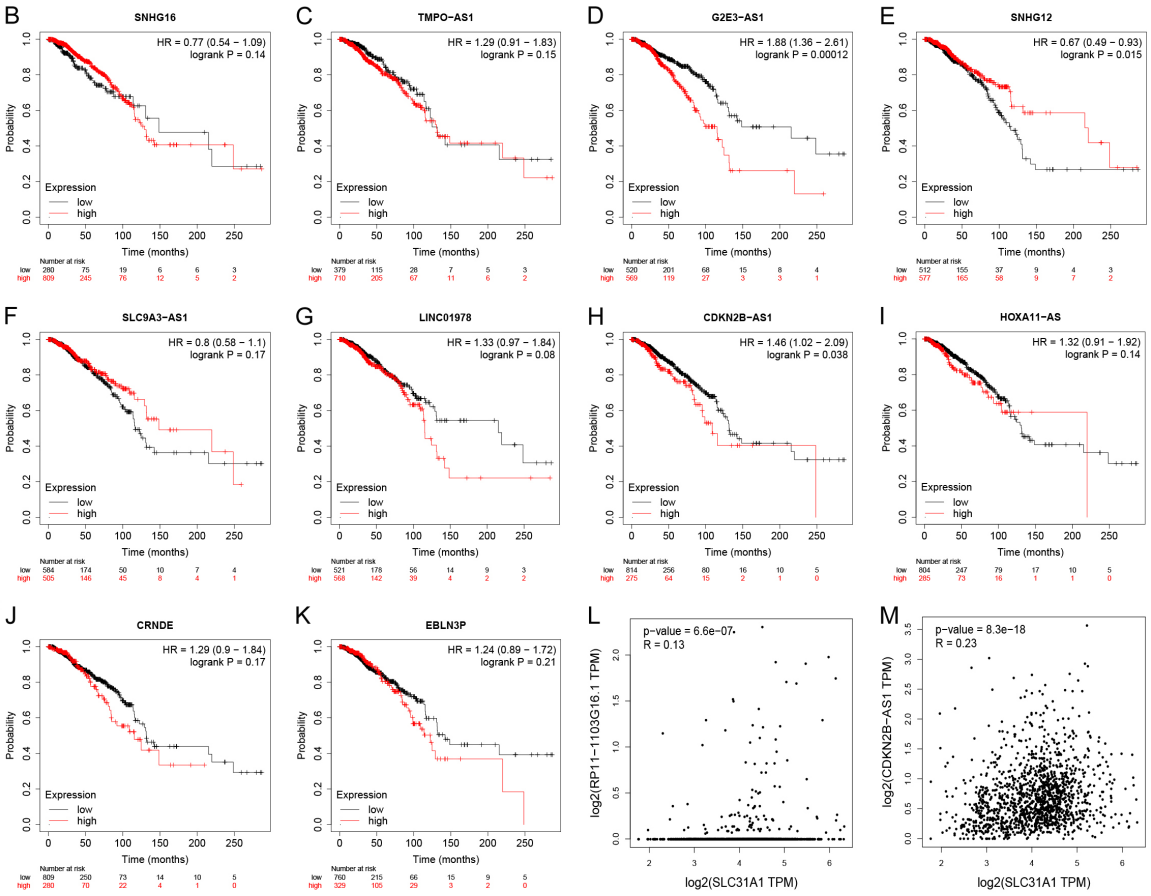

Figure 10. Expression analysis, survival analysis and correlation analysis for the potential upstream lncRNAs of miRNA/SLC31A1 axis in breast cancer. (A) The expression landscape of the potential lncRNAs in breast cancer determined by starBase. Red: high expression; green: low expression; grey: no statistical difference. The prognostic values of SNHG16 (B), TMPO-AS1 (C), G2E3-AS1 (D), SNHG12 (E), SLC9A3-AS1 (F), LINC01978 (G), CDKN2B-AS1 (H), HOXA11-AS (I), CRNDE (J) and EBLN3P (K) in breast cancer assessed by Kaplan-Meier plotter. The expression correlation of SLC31A1 with G2E3-AS1 (L) or CDKN2B-AS1 (M) in breast cancer determined by GEPIA.

tively linked to its copy number levels in breast cancer (**Figure 11A**). As shown in **Figure 11B**, SLC31A1 expression was generally upregulated with the increase of copy number, indicating that copy number might partially account for SLC31A1 expression in breast cancer. It has been widely acknowledged that promoter hypermethylation might lead to downregulation of gene expression. Thus, the promoter methylation of SLC31A1 in breast cancer was also determined using TCGA and METABRIC data. No statistical correlation of SLC31A1 expression with its promoter methylation level or significant differences between breast cancer and normal controls were observed as presented in **Figure 11C**, **11D**. The action mechanism graph of this study was vividly depicted in **Figure 12**.

Disclosure of conflict of interest

None.

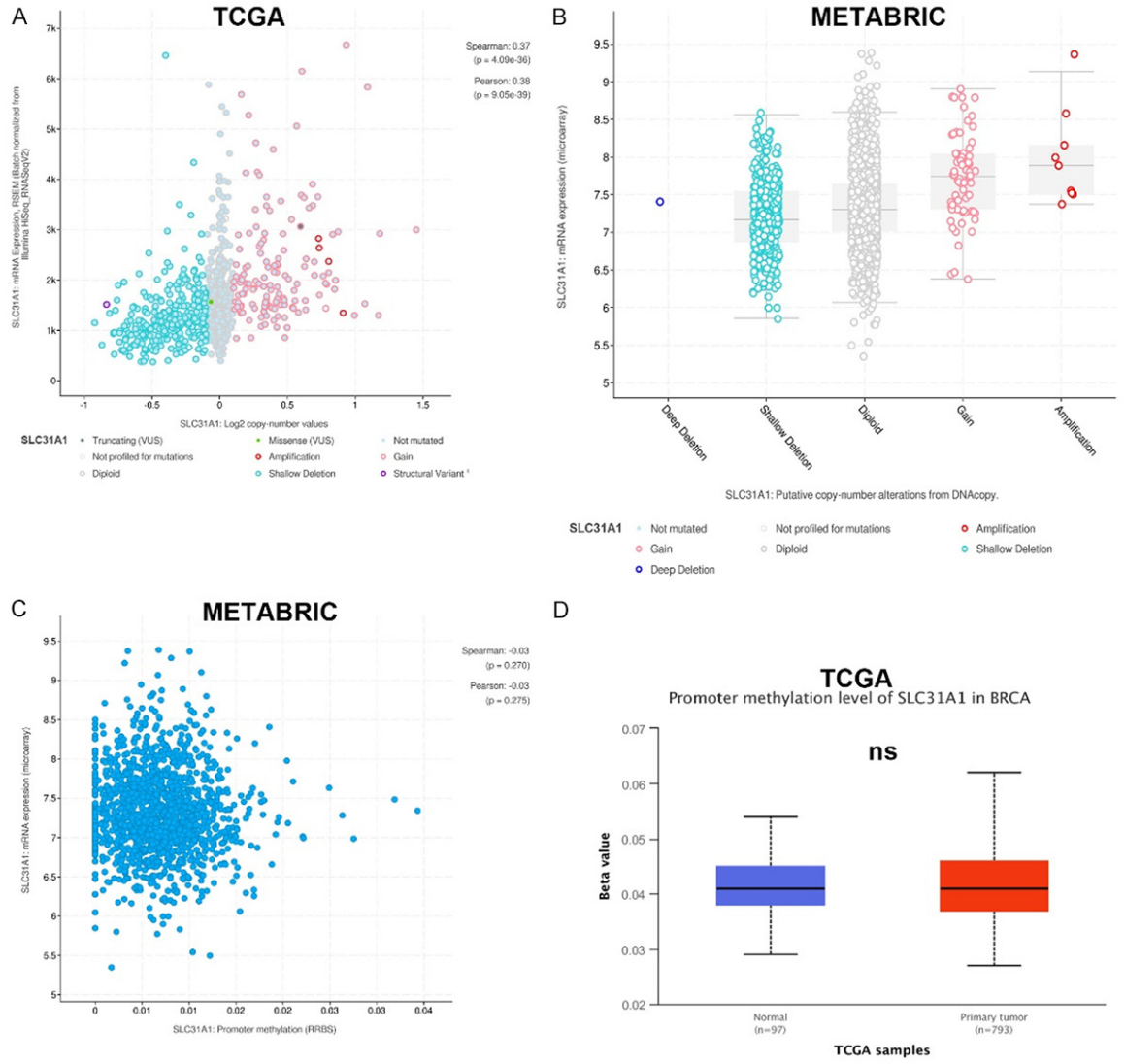

Figure 11. Analysis for the copy number alteration or promoter methylation level of SLC31A1 in breast cancer. The relationship of SLC31A1 mRNA expression with its copy number alterations in TCGA (A) or METABRIC (B) database. The relationship of SLC31A1 mRNA expression with its promoter methylation level in METABRIC (C) or TCGA (D) database. $^{ns}P>0.05$.

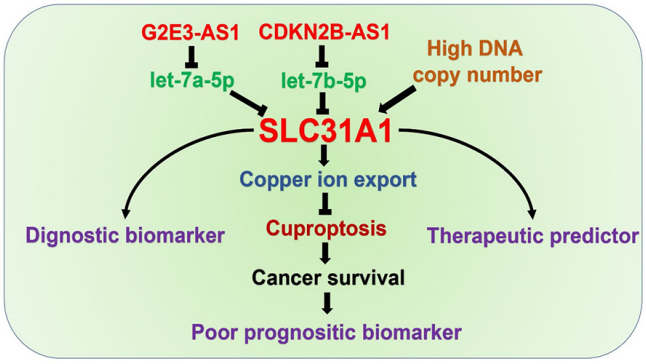

Figure 12. The model of cuproptosis-related SLC31A1's dysregulated and action mechanisms and its application values in breast cancer.

Address correspondence to: Linhang Mei, Department of Oncological Surgery, Taizhou Hospital of Zhejiang Province Affiliated to Wenzhou Medical University, Taizhou 317000, Zhejiang, China. E-mail: mlh0401297@126.com

References

[1] Sung H, Ferlay J and Siegel RL. Global cancer statistics 2020: GLOBOCAN estimates of incidence and mortality worldwide for 36

cancers in 185 Countries. CA Cancer J Clin 2021; 71: 209-249.
[2] Wang S, Jin J, Chen J and Lou W. MUC14-Related ncRNA-mRNA network in breast cancer. Genes (Basel) 2021; 12: 1677.
[3] Tsvetkov P, Coy S, Petrova B, Dreishpoon M, Verma A, Abdusamad M, Rossen J, Joesch-Cohen L, Humeidi R, Spangler RD, Eaton JK, Frenkel E, Kocak M, Corsello SM, Lutsenko S, Kanarek N, Santagata S and Golub TR. Copper induces cell death by targeting lipoylated TCA cycle proteins. Science 2022; 375: 1254-1261.
[4] Jiang Y, Huo Z, Qi X, Zuo T and Wu Z. Copper-induced tumor cell death mechanisms and antitumor theragnostic applications of copper complexes. Nanomedicine (Lond) 2022; 17: 303-324.
[5] Tao X, Wan X, Wu D, Song E and Song Y. A tandem activation of NLRP3 inflammasome induced by copper oxide nanoparticles and dissolved copper ion in J774A.1 macrophage. J Hazard Mater 2021; 411: 125134.
[6] Dong J, Wang X, Xu C, Gao M, Wang S, Zhang J, Tong H, Wang L, Han Y, Cheng N and Han Y. Inhibiting NLRP3 inflammasome activation prevents copper-induced neuropathology in a murine model of Wilson's disease. Cell Death Dis 2021; 12: 87.
[7] Yu Z, Zhou R, Zhao Y, Pan Y, Liang H, Zhang JS, Tai S, Jin L and Teng CB. Blockage of SLC31A1-dependent copper absorption increases pancreatic cancer cell autophagy to resist cell death. Cell Prolif 2019; 52: e12568.
[8] Chen GH, Lv W, Xu YH, Wei XL, Xu YC and Luo Z. Functional analysis of MTF-1 and MT promoters and their transcriptional response to zinc (Zn) and copper (Cu) in yellow catfish Pelteobagrus fulvidraco. Chemosphere 2020; 246: 125792.
[9] Tavera-Montañez C, Hainer SJ, Cangussu D, Gordon SJV, Xiao Y, Reyes-Gutierrez P, Imbalzano AN, Navea JG, Fazzio TG and Padilla-Benavides T. The classic metal-sensing transcription factor MTF1 promotes myogenesis in response to copper. FASEB J 2019; 33: 14556-14574.
[10] Wu G, Peng H, Tang M, Yang M, Wang J, Hu Y, Li Z, Li J, Li Z and Song L. ZNF711 down-regulation promotes CISPLATIN resistance in epithelial ovarian cancer via interacting with JHDM-2A and suppressing SLC31A1 expression. EBioMedicine 2021; 71: 103558.
[11] Zhang S, Guan X, Liu W, Zhu Z, Jin H, Zhu Y, Chen Y, Zhang M, Xu C, Tang X, Wang J, Cheng W, Lin W, Ma X and Chen J. YTHDF1 alleviates sepsis by upregulating WWP1 to induce NLRP3 ubiquitination and inhibit caspase-1-dependent pyroptosis. Cell Death Discov 2022; 8: 244.
[12] Fujita K, Motoyama S, Sato Y, Wakita A, Nagaki Y, Minamiya Y and Miura M. Effects of SLC31A1 and ATP7B polymorphisms on platinum resistance in patients with esophageal squamous cell carcinoma receiving neoadjuvant chemoradiotherapy. Med Oncol 2021; 38: 6.
[13] Bian Z, Fan R and Xie L. A novel cuproptosis-related prognostic gene signature and validation of differential expression in clear cell renal cell carcinoma. Genes (Basel) 2022; 13: 851.
[14] Oliveri V. Selective targeting of cancer cells by copper ionophores: an overview. Front Mol Biosci 2022; 9: 841814.
[15] Li SR, Bu LL and Cai L. Cuproptosis: lipoylated TCA cycle proteins-mediated novel cell death pathway. Signal Transduct Target Ther 2022; 7: 158.
[16] Cheng C, Ding Q, Zhang Z, Wang S, Zhong B, Huang X and Shao Z. PTBP1 modulates osteosarcoma chemoresistance to cisplatin by regulating the expression of the copper transporter SLC31A1. J Cell Mol Med 2020; 24: 5274-5289.
[17] Lou W, Wang W, Chen J, Wang S and Huang Y. ncRNAs-mediated high expression of SEMA3F correlates with poor prognosis and tumor immune infiltration of hepatocellular carcinoma. Mol Ther Nucleic Acids 2021; 24: 845-855.
[18] Chae YK, Arya A, Iams W, Cruz MR, Chandra S, Choi J and Giles F. Current landscape and future of dual anti-CTLA4 and PD-1/PD-L1 blockade immunotherapy in cancer; lessons learned from clinical trials with melanoma and non-small cell lung cancer (NSCLC). J Immunother Cancer 2018; 6: 39.
[19] Lou W, Chen J, Ding B and Fan W. XIAP, commonly targeted by tumor suppressive miR-3607-5p and miR-3607-3p, promotes proliferation and inhibits apoptosis in hepatocellular carcinoma. Genomics 2021; 113: 933-945.
[20] Lou W, Liu J, Ding B, Jin L, Xu L, Li X, Chen J and Fan W. Five miRNAs-mediated PIEZO2 down-regulation, accompanied with activation of Hedgehog signaling pathway, predicts poor prognosis of breast cancer. Aging (Albany NY) 2019; 11: 2628-2652.
[21] Bao JH and Li JB. Deciphering a novel necroptosis-related mirna signature for predicting the prognosis of clear cell renal carcinoma. Anal Cell Pathol (Amst) 2022; 2022: 2721005.
[22] Shi Y, Zhang Y, Ran F, Liu J, Lin J, Hao X, Ding L and Ye Q. Let-7a-5p inhibits triple-negative breast tumor growth and metastasis through GLUT12-mediated warburg effect. Cancer Lett 2020; 495: 53-65.
[23] Al-Harbi B, Hendrayani SF, Silva G and Aboussekhra A. Let-7b inhibits cancer-promoting effects of breast cancer-associated fibroblasts through IL-8 repression. Oncotarget 2018; 9: 17825-17838.

[24] Zhao Y, Yang F, Li W, Xu C, Li L, Chen L, Liu Y and Sun P. miR-29a suppresses MCF-7 cell growth by downregulating tumor necrosis factor receptor 1. Tumour Biol 2017; 39: 1010428317692264.
[25] Salmena L, Poliseno L, Tay Y, Kats L and Pandolfi PP. A ceRNA hypothesis: the Rosetta Stone of a hidden RNA language? Cell 2011; 146: 353-358.
[26] Karreth FA and Pandolfi PP. ceRNA cross-talk in cancer: when ce-bling rivalries go awry. Cancer Discov 2013; 3: 1113-1121.
[27] Xue C, Yi C, Lin H, Zhao J, Yuan J, Chen Y, Chen H, Lin L and Zhao Y. lncRNA CDKN2B-AS1 could be an indicator to identify prognosis and status of immune microenvironment in thyroid cancer. Dis Markers 2022; 2022: 4317480.
[28] Li Z, Cai X, Zou W and Zhang J. CDKN2B-AS1 promotes the proliferation, clone formation, and invasion of nasopharyngeal carcinoma cells by regulating miR-98-5p/E2F2 axis. Am J Transl Res 2021; 13: 13406-13422.
[29] Yang D, Ma J and Ma XX. CDKN2B-AS1 promotes malignancy as a novel prognosis-related molecular marker in the endometrial cancer immune microenvironment. Front Cell Dev Biol 2021; 9: 721676.
[30] Lu J, Chen Y, Wen L, Zhou Q and Yan S. LncRNA CDKN2B-AS1 contributes to glioma development by regulating the miR-199a-5p/DDR1 axis. J Gene Med 2022; 24: e3389.
[31] Qin S, Ning M, Liu Q, Ding X, Wang Y and Liu Q. Knockdown of long non-coding RNA CDKN2B-AS1 suppresses the progression of breast cancer by miR-122-5p/STK39 axis. Bioengineered 2021; 12: 5125-5137.
[32] Lu X, Wang J, Wang W, Lu C, Qu T, He X, Liu X, Guo R and Zhang E. Copy number amplification and SP1-activated lncRNA MELTF-AS1 regulates tumorigenesis by driving phase separation of YBX1 to activate ANXA8 in non-small cell lung cancer. Oncogene 2022; 41: 3222-3238.
[33] Wang W, Ding B, Lou W and Lin S. Promoter hypomethylation and miR-145-5p downregulation- mediated HDAC11 overexpression promotes sorafenib resistance and metastasis of hepatocellular carcinoma cells. Front Cell Dev Biol 2020; 8: 724.
[34] Li JH, Liu S, Zhou H, Qu LH and Yang JH. starBase v2.0: decoding miRNA-ceRNA, miRNA-ncRNA and protein-RNA interaction networks from large-scale CLIP-Seq data. Nucleic Acids Res 2014; 42: D92-97.
[35] Yang JH, Li JH, Shao P, Zhou H, Chen YQ and Qu LH. starBase: a database for exploring microRNA-mRNA interaction maps from Argonaute CLIP-Seq and Degradome-Seq data. Nucleic Acids Res 2011; 39: D202-209.
[36] Li C, Tang Z, Zhang W, Ye Z and Liu F. GEPIA2021: integrating multiple deconvolution-based analysis into GEPIA. Nucleic Acids Res 2021; 49: W242-W246.
[37] Lánczky A and Győrffy B. Web-based survival analysis tool tailored for medical research (KMplot): development and implementation. J Med Internet Res 2021; 23: e27633.
[38] Mizuno H, Kitada K, Nakai K and Sarai A. PrognoScan: a new database for meta-analysis of the prognostic value of genes. BMC Med Genomics 2009; 2: 18.
[39] Li R, Qu H, Wang S, Chater JM, Wang X, Cui Y, Yu L, Zhou R, Jia Q, Traband R, Wang M, Xie W, Yuan D, Zhu J, Zhong WD and Jia Z. CancerMIRNome: an interactive analysis and visualization database for miRNome profiles of human cancer. Nucleic Acids Res 2022; 50: D1139-D1146.
[40] Szklarczyk D, Gable AL, Nastou KC, Lyon D, Kirsch R, Pyysalo S, Doncheva NT, Legeay M, Fang T, Bork P, Jensen LJ and von Mering C. The STRING database in 2021: customizable protein-protein networks, and functional characterization of user-uploaded gene/measurement sets. Nucleic Acids Res 2021; 49: D605-D612.
[41] Liu Z, Liu J and Liu X. CTR-DB, an omnibus for patient-derived gene expression signatures correlated with cancer drug response. Nucleic Acids Res 2022; 50: D1184-D1199.
[42] Li T, Fan J, Wang B, Traugh N, Chen Q, Liu JS, Li B and Liu XS. TIMER: a web server for comprehensive analysis of tumor-infiltrating immune cells. Cancer Res 2017; 77: e108-e110.
[43] Gao J, Aksoy BA, Dogrusoz U, Dresdner G, Gross B, Sumer SO, Sun Y, Jacobsen A, Sinha R, Larsson E, Cerami E, Sander C and Schultz N. Integrative analysis of complex cancer genomics and clinical profiles using the cBioPortal. Sci Signal 2013; 6: pl1.
[44] Chandrashekar DS, Bashel B, Balasubramanya SAH, Creighton CJ, Ponce-Rodriguez I, Chakravarthi B and Varambally S. UALCAN: a portal for facilitating tumor subgroup gene expression and survival analyses. Neoplasia 2017; 19: 649-658.

A

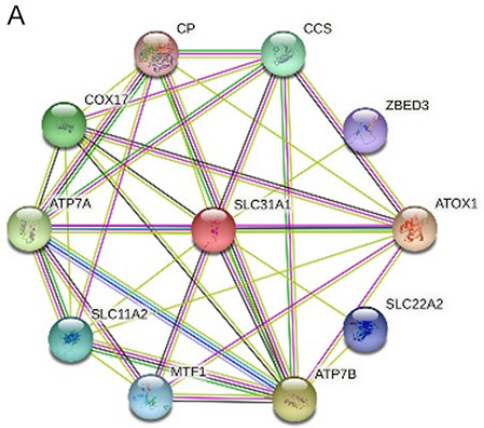

B

Biological Process (Gene Ontology)				
GO-term	description	count in network	strength	false discovery rate
GO:0060003	Copper ion export	3 of 3	3.25	3.08e-06
GO:0015680	Protein maturation by copper ion transfer	2 of 2	3.25	0.0010
GO:0035434	Copper ion transmembrane transport	5 of 6	3.17	5.72e-11
GO:0015677	Copper ion import	3 of 6	2.95	1.18e-05
GO:0006825	Copper ion transport	7 of 18	2.84	9.30e-15

C

Molecular Function (Gene Ontology)				
GO-term	description	count in network	strength	false discovery rate
GO:0043682	Copper transmembrane transporter activity, phosphorylative...	2 of 2	3.25	0.00070
GO:0016531	Copper chaperone activity	4 of 5	3.15	1.10e-08
GO:0005375	Copper ion transmembrane transporter activity	4 of 5	3.15	1.10e-08
GO:0032767	Copper-dependent protein binding	2 of 3	3.07	0.0010
GO:0016532	Superoxide dismutase copper chaperone activity	2 of 3	3.07	0.0010

Figure S1. The protein-protein interaction analysis and Gene Ontology analysis for SLC31A1-interacted proteins. A. The protein-protein interaction network of SLC31A1-interacted proteins. B. The top 5 enriched Biological Process (BP) items of SLC31A1-interacted proteins. C. The top 5 enriched Molecular Function (MF) items of SLC31A1-interacted proteins.